

1 **Separation of an upwelling current bounding the Juan
2 de Fuca Eddy**

3 **Jody M. Klymak^{1,2}, Susan E. Allen^{3,4}, Stephanie Waterman³**

4 ¹School of Earth and Ocean Sciences, University of Victoria, BC, Canada

5 ²Department of Physics & Astronomy, University of Victoria, BC, Canada

6 ³Department of Earth, Ocean and Atmospheric Sciences, University of British Columbia, Vancouver, BC,

7 Canada

8 ⁴Institute of Applied Mathematics, University of British Columbia, Vancouver, BC, Canada

9 **Key Points:**

- 10 • The shelf break current along Vancouver Island separates downstream of a submarine
11 bank.
- 12 • Offshore water is drawn onto the shelf and forms a sharp semi-persistent front with
13 the Juan de Fuca Eddy.
- 14 • The Eddy shows evidence of long residence times, and little evidence of deep-water
15 origin.

16 **Abstract**

17 Observations of temperature, salinity, and oxygen on the southern Vancouver Island
 18 shelf show a large-scale exchange of shelf water with offshore water, just offshore of a semi-
 19 permanent recirculation, often termed the Juan de Fuca Eddy. The Eddy occupies a region
 20 where the shelf widens abruptly in the lee of a bank. The water in this Eddy is a mixture
 21 of offshore water and water from a buoyant coastal current. This water is well-mixed along
 22 a mixing line in temperature-salinity space, though it retains stratification, and is either
 23 rapidly mixed or has a long residence time. There is a less than 1-km wide temperature-
 24 salinity front on the offshore side of this well-mixed water that has no sign of instabilities.
 25 The clearest evidence of cross-front transport is found during a tidally resolved survey over
 26 a bank. The transport is due to flows in the cross-bank direction that also drive 50-m tall
 27 hydraulic jumps. Upstream of the Eddy there is an along-shelf current flowing equatorward.
 28 However the whole current separates from the shelf before reaching the Eddy, in the lee of
 29 a bank, and is replaced by water from offshore. The separation event was also seen in sea-
 30 surface temperatures from satellite images as a tongue of cool coastal water that is ejected
 31 offshore.

32 **Plain Language Summary**

33 The southern Vancouver Island continental shelf is biologically productive due to high
 34 nutrient input from the Strait of Juan de Fuca and Salish Sea estuarine system and sub-
 35 stantial cross-shelf transport due to the complicated topography. Here we present intensive
 36 sampling of the Juan de Fuca Eddy region. The observations show that below the surface
 37 mixed layer, the water in the Eddy is low in oxygen, and has undergone substantial vertical
 38 and lateral mixing. In contrast to previous literature we find that the low oxygen in the
 39 Eddy is likely because of respiration rather than being pulled from low-oxygen water in the
 40 California Undercurrent.

41 The observations also show a remarkable flow separation of the equatorward shelf
 42 current. The current is seen to detach and is pushed offshore. Such events are readily seen
 43 in satellite imagery, but our observations indicate that the separation extends the depth of
 44 the water column on the shelf, and that this separation may be partially driven by the local
 45 bathymetry. The separation is a very strong cross-shelf exchange event, and transports
 46 substantial nutrient-rich coastal water offshore to drive productivity in the deeper ocean
 47 adjacent to the continental slope.

48 **1 Introduction**

49 Cross-shelf exchange is important to the health and productivity of continental shelf
 50 regions, allowing for offshore oxygenated water to be exchanged with nutrient-rich, but
 51 oxygen-depleted, nearshore water. Cross-shelf transport usually requires ageostrophic flow,
 52 since geostrophically balanced flow will tend to follow topographic contours, often providing
 53 a barrier to lateral exchange (Brink, 2016). Mechanisms of cross-shelf exchange include
 54 internal waves and instabilities in shelf-break fronts. However, these mechanisms can be
 55 smaller in magnitude compared to intermittent three-dimensional exchange, driven by ed-
 56 dying, often catalyzed by topographic irregularity (Barth et al., 2000).

57 Here we present detailed *in-situ* observations from the southern Vancouver Island shelf,
 58 collected in summer 2013, and sampled by a rapid profiling vehicle equipped with a CTD
 59 and oxygen sensor, supplemented by traditional hydrographic surveys bracketing the high
 60 resolution observations by a month. The shelf has complicated bathymetry (Fig. 1), with a
 61 relatively simple 50-km wide shelf poleward of our study site that widens to over 75 km wide
 62 equatorward of La Perouse Bank. The South Vancouver Island Shelf is this wide shelf region,
 63 characterized by a number of banks, and finally is incised on the equatorward side by the

64 Juan de Fuca Canyon. Water from the Strait of Juan de Fuca flows poleward as a buoyant
 65 current that hugs the coast (Thomson et al., 1989; Hickey et al., 1991), while shelf water
 66 flows equatorward in the summer both forced by local winds and via teleconnections with
 67 the long, homogenous shelves equatorward off Washington and Oregon (Hickey et al., 1991;
 68 Thomson & Krassovski, 2015; Engida et al., 2016). Trapped between these two currents
 69 is a region of relatively homogenous water that has been termed the Juan de Fuca Eddy
 70 (Freeland & Denman, 1982; Freeland & McIntosh, 1989; Foreman et al., 2008; MacFadyen
 71 & Hickey, 2010), denoted “EDDY” below.

72 A goal of our study was to understand how the EDDY persists and how it exchanges
 73 water properties with offshore water. We focus on water deeper than 50m, below the summer
 74 mixed layer, because this water is trackable with water mass properties, even though the
 75 EDDY is often studied from the point of view of the surface circulation (MacFadyen &
 76 Hickey, 2010). Past studies found low oxygen concentrations in the EDDY, and inferred
 77 that water is upwelled from the California Undercurrent from as deep as 400 m (Freeland
 78 & Denman, 1982; Dewey & Crawford, 1988). This inference was based on the assumption
 79 that oxygen is a conservative tracer, and hence water in the EDDY had to come from the
 80 oxygen minimum zone found further offshore (Mackas et al., 1987). It was hypothesized
 81 that the EDDY was fed by waters being drawn up a spur canyon (called the Spur Canyon)
 82 via ageostrophic transport from offshore to onshore due to low pressure in the EDDY center
 83 (Weaver & Hsieh, 1987). Below, we will argue that there is no evidence of such transport
 84 and that oxygen is likely low because of local consumption due to respiration.

85 A second goal of our study was to better understand cross-shore exchange between
 86 shelf and offshore water. For a two-dimensional topography with along-shore wind forcing,
 87 cross-shore transport is supplied by Ekman layers. However, in many locations there is also
 88 evidence of eddies, meanders, and filaments driving wholesale separation of shelf currents
 89 into the deep ocean. These have been well-studied off California (Strub et al., 1991) where
 90 satellite and *in-situ* observations show large meanders of coastal upwelling currents leading
 91 to coastal water injected into the offshore domain. Along the Vancouver Island shelf, large
 92 instabilities of the coastal current have also been inferred using satellite images (Ikeda &
 93 Emery, 1984; Thomson & Gower, 1998). Direct observations of such filaments have been
 94 made further to the south off Cape Blanco (Barth et al., 2000), and off other coasts (Relvas
 95 & Barton, 2005). Net cross-shore transport of nutrients and chlorophyll have been found in
 96 hydrographic surveys off Vancouver Island (Mackas & Yelland, 1999), and associated with
 97 mesoscale features in geostrophic velocities and in satellite observations. The mechanisms
 98 driving such separations are poorly understood, but hypotheses include coastal hydraulics
 99 leading to along-shore trapping of coastal waves (Dale & Barth, 2001), wind stress curl
 100 variations (Castelao & Barth, 2007), induced relative vorticity due to stretching of parcels
 101 that overshoot their initial isobaths due to a sudden change in downstream bathymetry
 102 (D’Asaro, 1988), and, at this location, non-linear breaking of large-scale meanders due
 103 to baroclinic instability between the wind-driven current and the California Undercurrent
 104 (Ikeda et al., 1984; Batteen, 1997).

105 In this paper we present observations of water masses on the Southern Vancouver Island
 106 Shelf collected in 2013 (section 2), presenting the data in a number of ways to highlight the
 107 important processes. We focus on the offshore side of the EDDY region (section 3) where
 108 we consider the age of the EDDY, the steadiness of the front separating the EDDY and the
 109 offshore water, properties along the Spur Canyon that was believed to feed the EDDY, and
 110 a large offshore tongue of the shelf-break current and its intrusion into the interior. We
 111 conclude by discussing the origin of the EDDY and the implications of the separating jet
 112 (section 4).

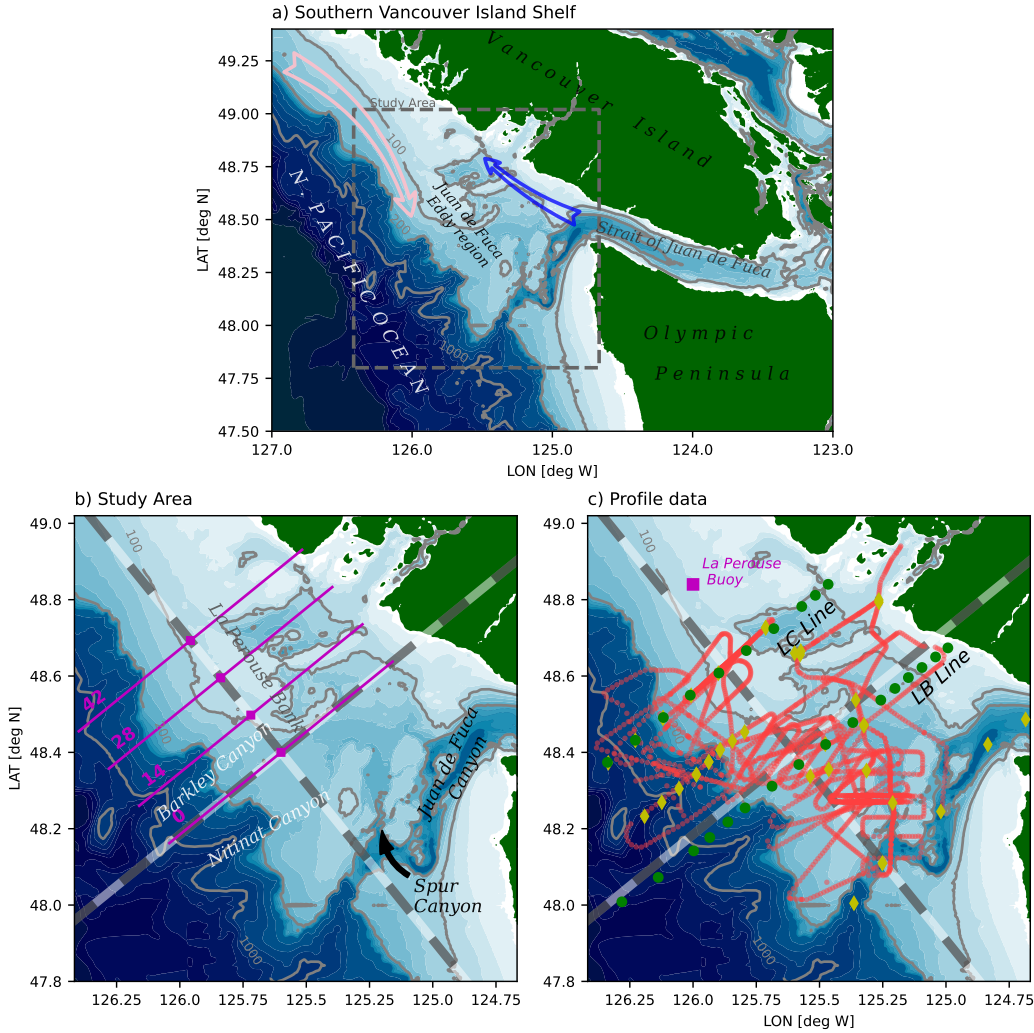


Figure 1. a) Study site on the Vancouver Island Shelf. The blue arrow indicates the direction of the Vancouver Island Coastal Current, and the pink arrow indicates southward flow of the coastal upwelling current. The dashed box indicates the approximate limits of the study area. b) The study area with major bathymetric features labelled. The coordinate system used for this paper is shown with alternating grey and white bands at 10-km intervals in the along- and cross-shore directions. c) sample locations with hydrographic casts from the La Perouse cruises along the LB and LC Lines (green dots), hydrographic casts during the Falkor cruise (yellow diamonds), and finescale Moving Vessel Profiler casts (red dots). Magenta square is La Perouse wind buoy.

113 **2 Site and Methods**

114 The study site was the southern portion of the Vancouver Island Shelf (Fig. 1a), a
 115 particularly complicated region due to the bathymetry and varied forcing. At the south end
 116 of the study site is the Juan de Fuca Canyon, which feeds dense water into Juan de Fuca
 117 Strait. This dense water is mixed with fresh water from the Fraser River at the sills and
 118 archipelagos further inland and fluxes out the Strait again, where it turns poleward along
 119 Vancouver Island to form the Vancouver Island Coastal Current. The Juan de Fuca Canyon
 120 has a notable spur canyon (Spur Canyon) that incises the shelf towards the north into the
 121 study site (Fig. 1b). The rest of the shelf is punctuated by a series of banks and shallow
 122 basins. La Perouse Bank separates the outer shelf from a deeper inner basin and forms the
 123 poleward boundary off where the shelf widens abruptly south of 48.5 N. Equatorward, the
 124 shelf widens further, and the shelf break has a series of submarine canyons, in particular
 125 Nitnat Canyon and Barkley Canyon.

126 We use an along/across-shelf co-ordinate system with an origin at 48.4°N and 125.6°W,
 127 with the across-shelf x oriented 39 degrees north of East (Fig. 1b, grey/white alternating
 128 lines). The projection is Cartesian with a central latitude at 48.4°N, which is sufficient for
 129 the limited geographic extents discussed here.

130 Observations from La Perouse hydrographic surveys along the LB and LC lines, col-
 131 lected aboard the *CCGS Tully* from 2013-05-30 to 2013-05-31 (“May”), and 2013-09-07 to
 132 2013-09-09 (“September”) are used to put finescale observations in context of routine hy-
 133 drographic work in the study region. These lines span the 50 m isobath to deep offshore,
 134 with casts every 7.5 km across shelf. The data comes from a lowered Seabird 9-11 CTD,
 135 with an SBE 43 oxygen sensor.

136 The focus in this paper is on finescale surveys carried out between these hydrographic
 137 surveys, from 2013-08-21 to 2013-08-30. Data were collected from the *R/V Falkor* with an
 138 AML Oceanographic Moving Vessel Profiler (MVP). Data was collected analogously to data
 139 collected during similar field campaigns (Klymak et al., 2015, 2016; D’Asaro et al., 2018).
 140 The MVP was equipped with an AML Oceanographic CTD, and a Rinko Oxygen sensor
 141 with a 7-s response time foil. The MVP profiled to depths of 200 m or to within 5 m of
 142 the seafloor, whichever was shallower, and dropped at a speed of approximately 3 m s^{-1} .
 143 Data collection took place while the ship cruised at speeds between 5 and 8 kts, usually at
 144 around 6 kts, to enable fine horizontal spacing of the casts, with typical spacing of 800 m
 145 in deep water, and less in water shallower than 200 m. Data is reported for the downcast,
 146 which mostly follows a vertical path. The rapid speed of the profiling makes the oxygen
 147 measurements somewhat coarse, and probably biased due to the phase lag of the sensor, so
 148 we treat these qualitatively in this paper.

149 Unfortunately, neither vessel had an operational acoustic Doppler profiler during the
 150 cruises with which to make water velocity measurements.

151 Winds during the cruises were typical for the west coast of Vancouver Island, with
 152 equatorward upwelling-favorable winds during July and early August (Fig. 2). During the
 153 finescale survey, and for the week previous, the winds were intermittently downwelling fa-
 154 vorable. Note that this locale is strongly affected by coastally trapped waves from further
 155 south, so doming of near-bottom isopycnals often persists despite local wind forcing, and
 156 takes a finite amount of time to spin down (Thomson & Krassovski, 2015; Engida et al.,
 157 2016).

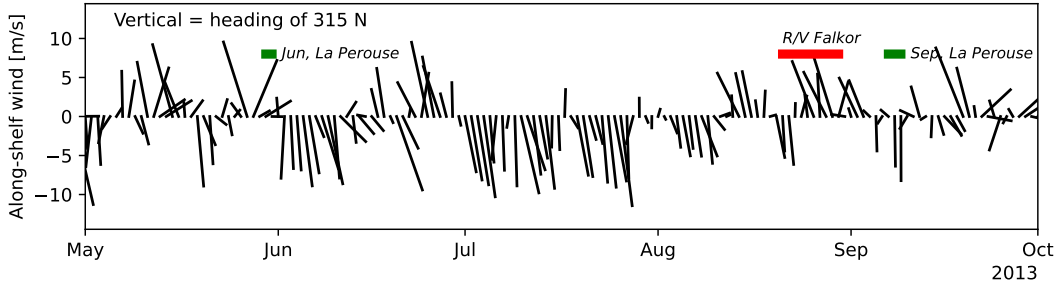


Figure 2. Wind from the La Perouse buoy at 48.84 N, 126 W (DFO, 2022). The vertical direction is along-shelf (chosen as a heading of 315 N), so vectors pointing straight down represent upwelling winds. The wind components have been low-pass filtered to one-day averages. The timing of the surveys discussed in the paper are shown as colored bands.

3 Observations

3.1 Early and late summer hydrographic surveys

Hydrographic sections along the LB and LC hydrographic lines highlight summer conditions on the Southern Vancouver Island Shelf and are presented to give context to the more detailed survey carried out on the *R/V Falkor* (Figure 3). During both surveys, and along both lines, there is clear evidence of upwelling, with the 26.4 kg m^{-3} isopycnal reaching from 130 m depth offshore to shallower than 85 m over the shelf. The upwelled water tends to be low in oxygen and cool. Further onshore, the Vancouver Island Coastal Current hugs the coast, where isopycnals tilt down towards the shore, and water is warmer than offshore.

The Juan de Fuca Eddy region is observed along the LB Line (Fig. 3, bottom three rows), mostly inshore of 0 km. The water in the EDDY is cooler and lower in oxygen than along the same isopycnal further offshore. Near the surface, the isopycnals are domed, and the low-oxygen anomaly extends as high as the thin surface mixed layer.

The water upstream of the EDDY region, along the LC line, is less mixed and has higher oxygen than the EDDY water (Fig. 3, top three rows). Based on these properties, offshore water does not appear to make it over La Perouse Bank into the onshore basin, or if it does, it does so intermittently and with substantial mixing. Note that the water along the 26.4 kg m^{-3} isopycnal (Fig. 3, magenta contours) becomes cooler and lower in oxygen where it intersects the shelf, consistent with both enhanced mixing near the shelf and with drawdown of oxygen by respiration.

The contrast in onshore and offshore waters can be clearly traced in temperature-salinity (θ -S) anomalies along isopycnals (Fig. 4a). Denser than 26.6 kg m^{-3} , the deep water masses found offshore are largely homogenous. In the lighter water masses, there are distinct differences between warm and salty offshore water compared to water on the shelf at the same densities.

We use a spice anomaly defined as relative to a straight line in θ -S space (Fig. 4) representing an approximate mixing line for water in the EDDY, and passing through the points 7.75°C , 30 psu and 6.6°C , 35 psu. Spice anomaly for a given water sample at density σ_θ is given by $\gamma = \alpha(T - T_0(\sigma_\theta)) + \beta(S - S_0(\sigma_\theta))$ where $T_0(\sigma_\theta)$, $S_0(\sigma_\theta)$ are the temperature and salinity along the mixing line at the same density as the water sample. The sign convention is that a positive anomaly is warmer and saltier than data along the mixing line.

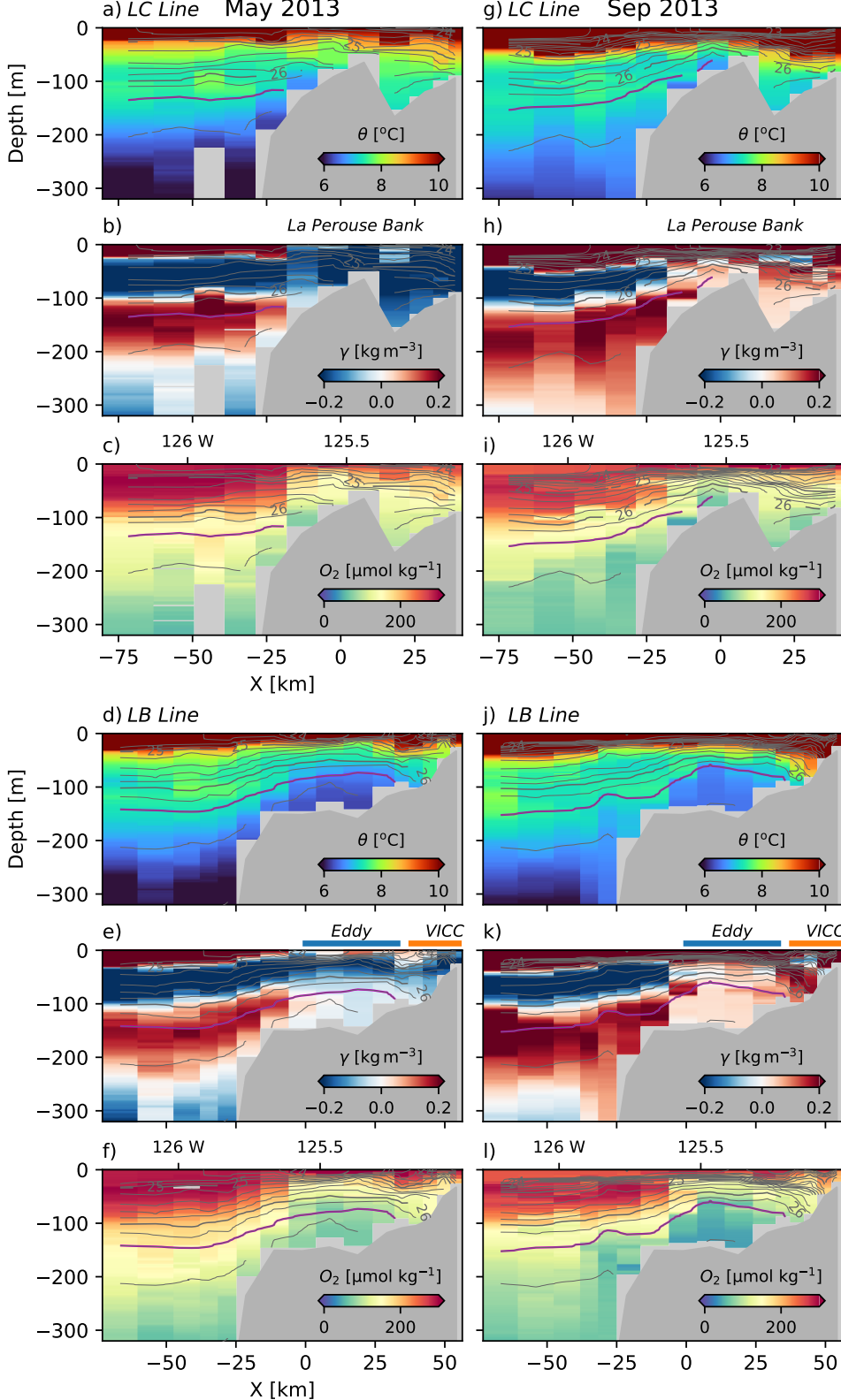


Figure 3. Observations along LC Line in May (a–c) and Sep (g–i) and LB lines in May (d–f) and Sep (j–l). X is across-shelf distance in the coordinate system shown in Fig. 1. Potential density is contoured every 0.2 kg m⁻³, with the 26.4 kg m⁻³ colored magenta. Potential temperature, θ , splice anomaly, γ and oxygen concentration, O_2 , are colored for each section.

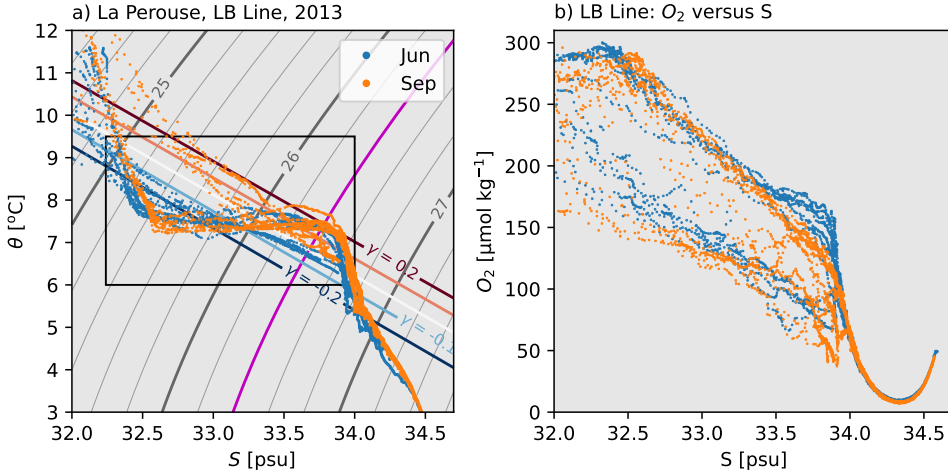


Figure 4. a) Potential temperature, θ , versus salinity, S , for the La Perouse data shown in Fig. 3; potential density is contoured every 0.2 kg m^{-3} , with the 26.4 kg m^{-3} colored magenta. A definition of spice anomaly is shown in this plot, and discussed in the text. The rectangle is the $\theta - S$ range used in Fig. 5 below. b) The same data with oxygen concentration versus salinity.

Using this metric of spice anomaly, offshore water tends to have high absolute values (Fig. 3, middle rows), with a positive-anomaly layer ($\gamma \approx 0.2 \text{ kg m}^{-3}$, red colors) centered at 26.4 kg m^{-3} sandwiched between negative-anomaly layers above and below. On the shelf ($-10 \text{ km} < X < 30 \text{ km}$), the distinct $\theta - S$ masses are attenuated and much closer to the defined mixing line than the offshore water ($\gamma \approx 0 \text{ kg m}^{-3}$, almost white Fig. 3).

There are temporal changes over the summer. Away from the surface, water has upwelled from deeper depths by September, but the offshore water maintains the same water mass characteristics through the summer. Hugging the coast ($X > 30 \text{ km}$), the Vancouver Island Coastal Current warms during the summer, and the spice anomaly goes from negative to positive. In the EDDY, the water stays near the mixing line, but is cooler in the spring (Fig. 3, LB Line, left-hand column: slightly negative spice anomaly) and warms during the summer (Fig. 3, LB Line, right-hand column: slightly positive spice anomaly).

Oxygen concentration in both surveys has a similar dichotomy between the EDDY and off-shelf water. Water found in the EDDY has oxygen concentrations $100 \mu\text{mol kg}^{-1}$ lower on the shelf than off-shelf (Fig. 3, Fig. 4b). The very deepest water ($S \approx 33.9 \text{ psu}$) on the shelf shows a further $50 \mu\text{mol kg}^{-1}$ decrease in concentration between May and September along the LB line.

3.2 Finescale surveys

3.2.1 Overview

The finescale surveys covered most of the EDDY region, with an emphasis on the offshore edge near the shelfbreak front (Fig. 1). For water denser than 26 kg m^{-3} , there are three distinct water masses sampled on the shelf (Fig. 5). The first is offshore water, which tends to be warmer, and hence has a positive spice anomaly ($\gamma \approx 0.2 \text{ kg m}^{-3}$ along $\sigma_\theta = 26.4 \text{ kg m}^{-3}$). The second is water in the EDDY, which during this survey was found along the straight mixing line in $\theta - S$ space (Fig. 5, $\gamma \approx 0 \text{ kg m}^{-3}$ along $\sigma_\theta = 26.4 \text{ kg m}^{-3}$). Between these two water masses, there is a less populous mass (Fig. 5, $\gamma \approx 0.1 \text{ kg m}^{-3}$ along $\sigma_\theta = 26.4 \text{ kg m}^{-3}$) that we demonstrate below is found on the shelf poleward of the EDDY.

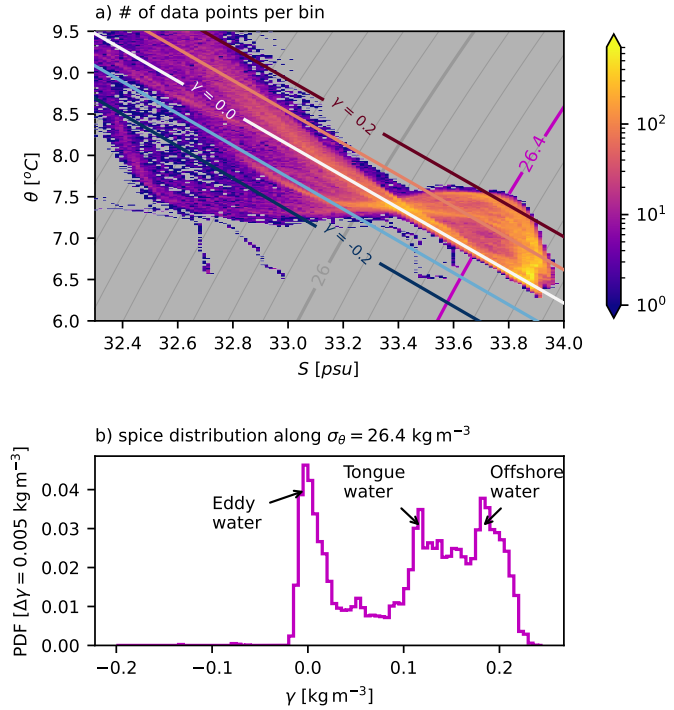


Figure 5. a) Binned sample density of salinity and potential temperature from the cruise, with a logarithmic color scale. Grey contours are potential density relative to the surface at intervals of 0.1 kg m^{-3} ; the magenta contour is the 26.4 kg m^{-3} isopycnal. Colored contours are spice anomaly, γ , relative to the white line labeled $\gamma = 0.0$. b) Distribution of spice, γ along the 26.4 kg m^{-3} isopycnal.

In synthetic cross sections of spice anomaly, the EDDY is clearly identifiable as having low spice anomaly ($\gamma \approx 0 \text{ kg m}^{-3}$, Fig. 6c, d). These lines are made with a two-dimensional interpolation where MVP casts at a given depth are given a Gaussian weight $w = e^{-(r/r_0)^2}$, where r is the distance from the line and $r_0 = 1.5 \text{ km}$. Note that the section at The low-spice anomaly water extends from the seafloor to approximately 30 m depth, onshore of $X \approx 0 \text{ km}$. Despite lying along a mixing line, the EDDY water is still stratified. The high-spice water ($\gamma \approx 0.2 \text{ kg m}^{-3}$) is found offshore of the EDDY water, on the other side of a sharp $\theta - S$ compensated front. This front is even sharper in individual sections than in these composite sections (see section 3.2.3).

In contrast, the third population of partially mixed water between the EDDY and offshore water (Fig. 5) is all found poleward of the EDDY region (Fig. 6a, b) as water with a weaker spice anomaly ($\gamma \approx 0.1 \text{ kg m}^{-3}$, pink colors). This water is not as warm as offshore water, indicating some mixing with offshore water has taken place. Of note is that this intermediate water mass appears completely absent in the sections further equatorward (Fig. 6c, d), indicating that it is either mixed away or that it is advected elsewhere; we argue below that it is advected offshore in a large-scale tongue.

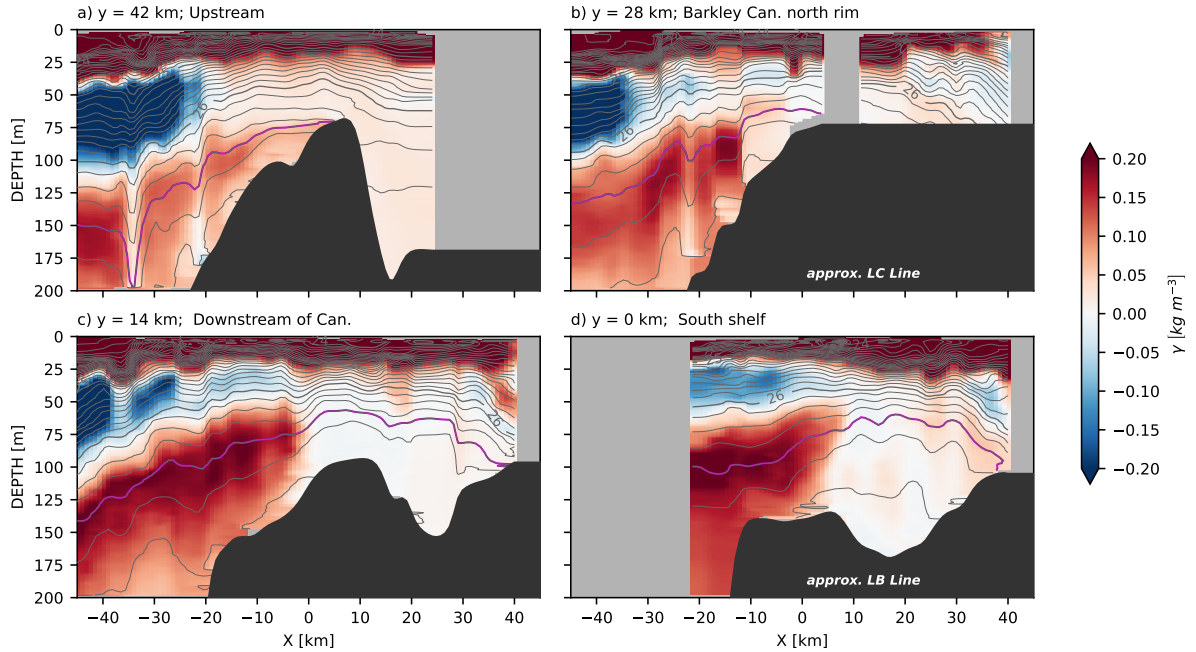


Figure 6. Synthetic sections of spice anomaly from the MVP data, projected along four lines from poleward (upstream of coastal current) a) to equatorward (downstream); the lines are shown in Fig. 1a). Isopycnals are contoured every $\sigma_\theta = 0.2 \text{ kg m}^{-3}$, with the $\sigma_\theta = 26.4 \text{ kg m}^{-3}$ isopycnal highlighted in magenta. Colors are spice anomaly as defined in Fig. 5. "BC" in panel (c) refers to Barkley Canyon. Note that b) is along LC line (Fig. 3a–c,g–i), and d) is along the LB line (Fig. 3d–f,j–l).

Oxygen saturation sections show that the deep water in the EDDY has very low oxygen saturation (Fig. 7c, d) compared to surrounding water (though again, we caution against the quality of these saturation values from such a fast profiling instrument with a slow response time). More oxygenated water is found offshore, and the oxygen deficit is not as strong in the poleward sections (Fig. 7a, b). The T/S compensated front also shows an abrupt

239 transition from the EDDY water and the offshore. Note the excellent correlation between
 240 oxygen saturation and spice anomaly in Fig. 6.

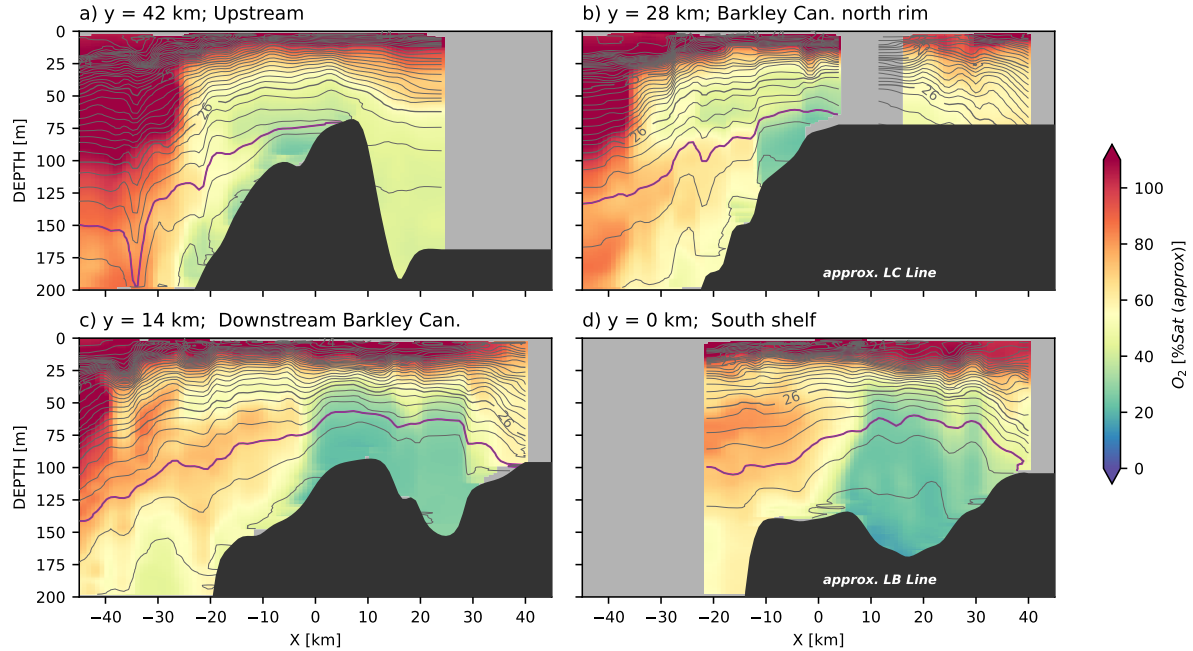


Figure 7. As in Fig. 6, for oxygen approximate saturation.

241 The spatial patterns are very clear when considering a map view of properties along
 242 the $\sigma_\theta = 26.4 \text{ kg m}^{-3}$ isopycnal (Fig. 8). There is a region onshore of the south tip of La
 243 Perouse Bank (approximately $48.5^\circ\text{N}, 125.75^\circ\text{W}$), that consists of water that is found along
 244 the mixing line (spice anomaly $\gamma \approx 0 \text{ kg m}^{-3}$) that also has low oxygen saturation.
 245 Offshore of this region is water that is very warm and salty in comparison ($\gamma > 0.15 \text{ kg m}^{-3}$), and
 246 relatively high in oxygen (saturations of approximately 60%). The transition between these
 247 two water masses is very abrupt, and stretches from La Perouse Bank to a shallow bank
 248 just above the Juan de Fuca Canyon (48.3°N and 125.4°W).

249 Poleward of La Perouse bank and Barkley Canyon, the water along the shelf has the
 250 weaker spice anomaly characteristic of the third water mass ($\gamma \approx 0.1 \text{ kg m}^{-3}$, light pink
 251 colors). This water is also somewhat lower in oxygen than water from offshore, though
 252 not as depleted as the water in the EDDY. The water appears to be pushed offshore just
 253 upstream of Barkley Canyon and replaced on the shelf by the warmer (high spice) offshore
 254 water.

255 The correspondence between low oxygen water and water on the mixing line that
 256 defines $\gamma \approx 0 \text{ kg m}^{-3}$ is quite strong (Fig. 8c). Eddy water is onshore (more red colors), low
 257 in oxygen, and along the mixing line. Offshore water is high in oxygen and has a high spice
 258 anomaly. Water that is found poleward on the shelf is still relatively high oxygen, but of
 259 intermediate spice $\gamma \approx 0.125 \text{ kg m}^{-3}$.

260 3.2.2 Spur Canyon

261 The Spur Canyon leading from the Strait of Juan de Fuca has been implicated in allowing
 262 dense water to be upwelled into the EDDY (Mackas et al., 1987; Weaver & Hsieh, 1987).
 263 The sea surface is low in the middle of the EDDY, so it has been hypothesized that water

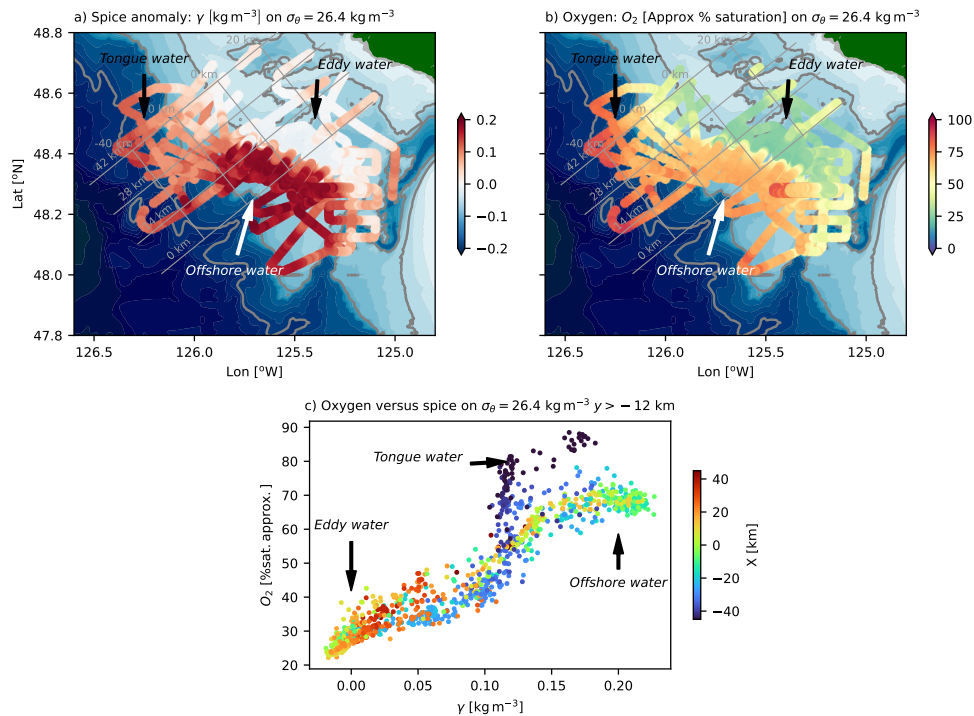


Figure 8. Spatial overview of a) the spice anomaly, and b) oxygen saturation on the $\sigma_\theta = 26.4 \text{ kg m}^{-3}$ isopycnal. Grey cross-slope lines are cross sections indicated in Fig. 6. Along-slope grey lines are every 20 km in the cross-slope direction, with $X = 0 \text{ km}$ near the 100-m isobath at the north end of the observation area. c) distribution of oxygen as a function of spice anomaly and $\sigma_\theta = 26.4 \text{ kg m}^{-3}$, colored by x-coordinate. Data from the Juan de Fuca Canyon region ($y < -12 \text{ km}$) is not shown.

moves up the Spur Canyon due to ageostrophic motion (Weaver & Hsieh, 1987; Freeland & Denman, 1982). It is difficult to infer flow up the Spur Canyon from the observations collected here. Three transects up the canyon indicate that deep isopycnals slope up into the canyon (Fig. 9, to approximately 30 km). Continuing across the EDDY, isopycnals are largely flat until they intersect the Vancouver Island Coastal Current ($X_{canyon} = 80$ km). The deeper isopycnals are not found in the deeper basin northeast of La Perouse Bank (70 km), thus the bank is a natural poleward boundary of the EDDY.

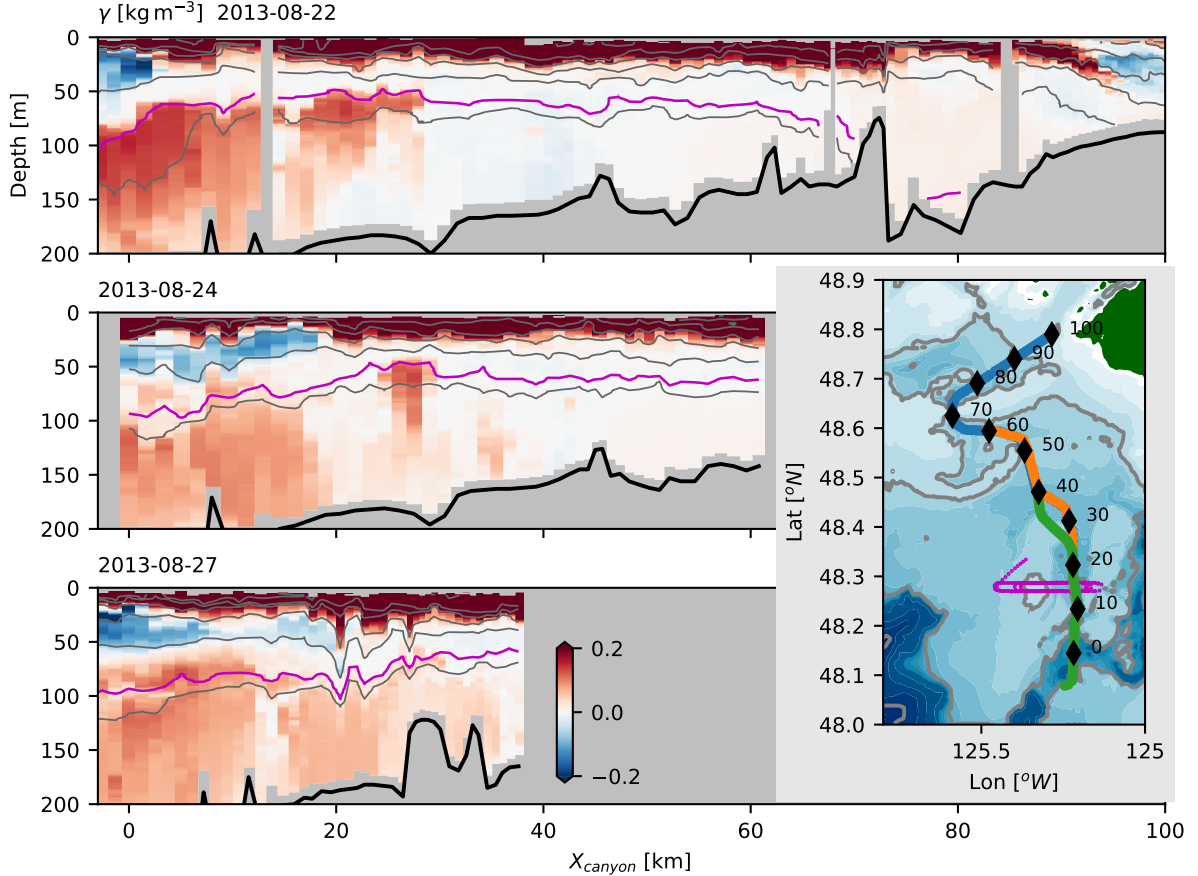


Figure 9. Spice anomaly surveys up the Spur Canyon, where X_{canyon} is along-canyon as defined in the map. Grey isopycnals are contoured every 0.5 kg m^{-3} , and the 26.4 kg m^{-3} isopycnal is shown in magenta. The seafloor is indicated with the thick black line. Map (lower right) shows the path taken during each survey in chronological order (blue, orange, and green). Magenta line is path taken during a cross-canyon survey (Fig. 10).

Spice anomaly along the canyon indicates a transition from offshore water to EDDY water. Oxygen saturation behaves in a similar manner, though some of the incoming water has slightly lower oxygen than water inside the EDDY (not shown). Based on these sections, it is difficult to infer water motion up the canyon.

Much of the modified water in the Spur Canyon appears to come from the shelf to the west, but heavily modified by tidal mixing. A repeat tidal survey over the bank on the west side of the canyon shows a strong hydraulic response during onshore flow (17:58–21:00, Fig. 10). Dense water passes from the offshore side into the canyon, and plunges down the side wall before rebounding downstream. Note that the tide here is largely diurnal, so

this onslope flow only occurs once a day. Given the stratification of $N \approx 6 \times 10^{-3} \text{ rad s}^{-1}$ and an overturning scale of 50 m, we might expect dissipation rates reaching $\epsilon \sim L^2 N^3 \approx 5 \times 10^{-4} \text{ m}^2 \text{s}^{-3}$, which is three orders of magnitude higher than dissipation observed on the shelf west of this location by Dewey and Crawford (1988). This estimate of turbulence dissipation rate implies a diapycnal diffusivity of $\kappa = \gamma \epsilon / N^2 \approx 0.5 - 5 \text{ m}^2 \text{s}^{-1}$, assuming a mixing efficiency of $\gamma = 0.2$. Water spills over from the offshore front into the canyon during the onshore tide. This water is rapidly mixed with surrounding water such that its strong offshore spice values are attenuated.

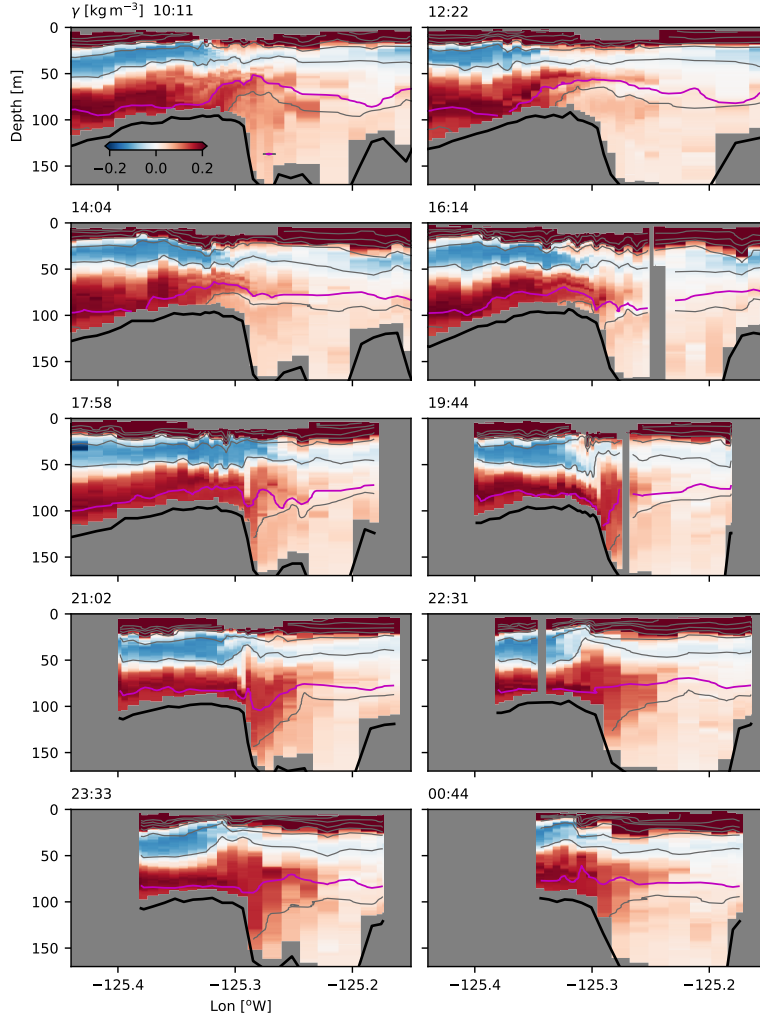


Figure 10. Spice anomaly observed in repeated, tide-resolving survey across the Spur Canyon, time is indicated in the upper left of each plot (29 August, 2013). Location of survey shown in Fig. 9 as a magenta line.

The turbulence found on the canyon rim makes it ambiguous if there is water moving up the canyon or not. There is a general tendency along the canyon for higher spice water to be found offshore (Fig. 9) but it seems likely that the source of the higher spice water is from over the bank rather than water being advected up the canyon. The tidally driven flow over the bank is the most significant source of high-spice offshore water into the EDDY region identified during our surveys.

294 ***3.2.3 Frontal survey***

295 A systematic survey through the front between the offshore water and the EDDY water
 296 demonstrates the sharpness and persistence of this front (Fig. 11), suggesting that it has
 297 limited exchange with the offshore region.

298 The survey started close to shore, and passed through the Vancouver Island Coastal
 299 Current (along-track 0–10 km). The coastal current forms a buoyant current, and is fresher
 300 and colder than water at the same density. The front with the coastal water is relatively
 301 thick, greater than 20 km wide, and has entrained partially mixed water down from the
 302 surface to the foot of the front ($\gamma \approx 0.1$).

303 Offshore of this coastal current, measurements were collected crossing the front be-
 304 tween the offshore water and the EDDY water 10 times, showing its evolution following the
 305 along-shore equatorward flow. First, as noted in the composite sections, isopycnals slope
 306 up from offshore onto the shelf. In the first crossing, the front is very sharp, (along-track
 307 distance 50 km) though two small tendrils of higher spice water can be seen separating from
 308 the front on the inshore side. Similar tendrils are found on the second crossing, perhaps a
 309 bit more separated from the front (≈ 80 km), and on the third crossing (≈ 95 km). These
 310 tendrils are made of up partially mixed water. The subsequent passes have more of this
 311 partially mixed water, such that the partially mixed front is up to 5-km wide by the fifth
 312 pass (≈ 150 km). However, the deeper isopycnals retain a sharp front, and indeed the front
 313 appears sharp again by the seventh pass at all depths (≈ 200 km).

314 There is evidence of some warmer water swirling into EDDY, particularly along isopyc-
 315 nals deeper than 26.4 kg m^{-3} . Regions of warmer (and more oxygenated) water are found
 316 in tendrils at these depths (e.g. ≈ 170 km and ≈ 185 km). The overall effect is similar to
 317 what was seen in the Gulf Stream with similar observations (Klymak et al., 2016); there
 318 are two quite distinct water masses, the EDDY water and the offshore water, as seen in
 319 the θ – S plot (Fig. 11c) with only a small population of samples between these two. These
 320 distinct θ – S properties are indicative of substantial isopycnal and vertical mixing, but even
 321 these populations are relatively cut off from the main water masses, indicating that they are
 322 well-mixed on their own, in short episodic events. Regardless, this front is very sharp given
 323 that it has no density signature, indicating that there is not strong advection from offshore
 324 into the EDDY region.

325 ***3.3 Separation of coastal water***

326 Upstream of the the sharp front between the low-spice EDDY and the high-spice off-
 327 shore water is a substantial mass of intermediate-spice water along the shelf (compare Fig. 6a
 328 and c). This intermediate spice water is moving equatorward along the shelf upstream of
 329 the EDDY, but is pushed offshore just upstream of Barkley Canyon (Fig. 12d). There is
 330 a tongue of intermediate-spice water ($\gamma \approx 0.1 \text{ kg m}^{-3}$, pink along 26.4 kg m^{-3}) that sepa-
 331 rates from the shelf just west of 126°W . The surveys do not cross the full extent of the
 332 tongue, but it is at least 30 km wide. It also appears to end at approximately 48.2°N . This
 333 intermediate-spice water reaches from relatively shallow isopycnals to at least 26.55 kg m^{-3}
 334 (Fig. 12h). Unfortunately, we cannot track the fate of this water mass because isopycnals
 335 tilt down offshore, below the depth limit of the MVP. The 25.8 kg m^{-3} isopycnal appears
 336 to have the tongue (Fig. 12a), but closer to the shelf than at 26.4 kg m^{-3} , indicating strong
 337 three-dimensionality to this feature.

338 This separating tongue is embedded in the larger scale isopycnal tilt caused by the
 339 upwelling (Fig. 12, c,f, and j), so it is difficult to see dynamically what is driving this offshore
 340 push. If the offshore motion were geostrophically balanced, we would expect the isopycnals
 341 to dome upwards from poleward towards Barkley Canyon, but if such doming is happening,
 342 it is weaker than variability from internal tides and synoptic unsteadiness. One possibility
 343 is that it is simple flow separation caused by the water not being able to make the sharp

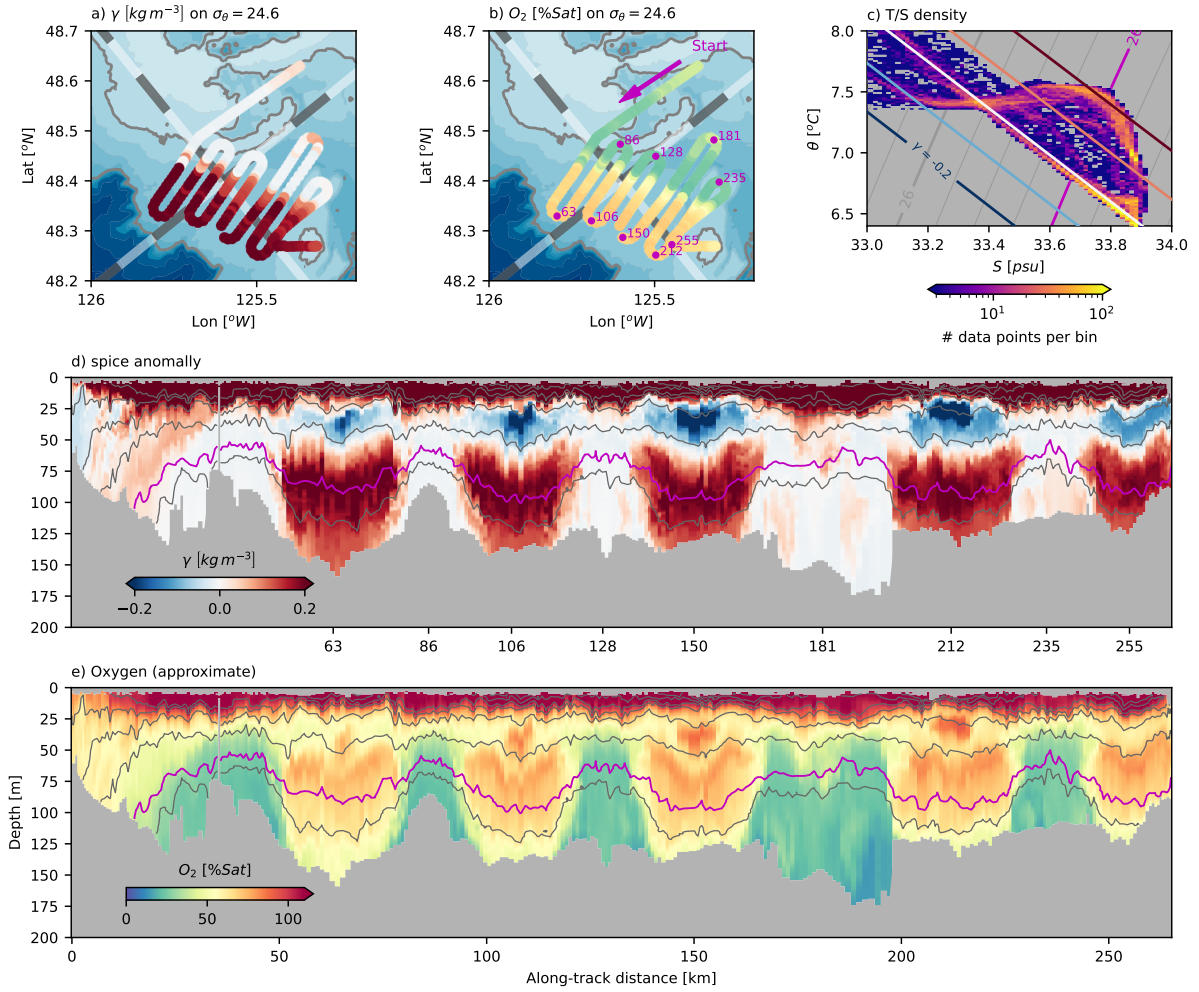


Figure 11. Data from the offshore front survey a) spice anomaly along 26.4 kg m^{-3} . Grey-white alternating lines are the coordinate system, with 10-km alternating shades. b) oxygen saturation along 26.4 kg m^{-3} ; magenta dots correspond to turn locations as distance along-track. c) density of data points (logscale) in this section of data. d) cross-section of spice anomaly along track. Grey isopycnals are contoured every 0.5 kg m^{-3} , and the 26.4 kg m^{-3} isopycnal is shown in magenta. Ticks are turn locations e) cross-section of oxygen saturation.

344 turn around La Perouse Bank, which would be an ageostrophic effect. Whatever causes it,
 345 downstream of the separation, the water is replaced by offshore water with much higher
 346 spice values. The high-spice water comes onto the shelf through much of the water column,
 347 so is not just being carried onshelf by near-bottom Ekman layer by wind driven upwelling.

348 There is a clear surface expression of the separating tongue in satellite imagery (Fig. 13).
 349 Water flowing equatorward along the shelf tends to be cooler than offshore water, likely due
 350 to mixing with the colder coming out of the Strait of Juan de Fuca. On August 25, there
 351 is a cold tongue of water separating from La Perouse Bank, crossing isobaths and pointing
 352 south at 125.8°W. There is a cooler tendril streaming west at 48 N off the south end of
 353 this tongue. This feature is not as well-developed in the previous image (Aug. 21) perhaps
 354 indicating that it is an evolving feature. By 31 August, there is no surface expression of
 355 the feature, though small tendrils of cooler water can be seen separating from La Perouse
 356 Bank. By 5 September, the water has significantly warmed, and the offshore anomaly does
 357 not appear to have a surface signature.

358 Satellite-based surface chlorophyll estimates show the same feature (Fig. 14) suggesting
 359 the advection of high chlorophyll to the west side of the EDDY. They also show a relatively
 360 high-chlorophyll tendril to the west, again exiting the study region at approximately 48
 361 degrees N. The feature is relatively long-lived, on the order of one month. Inspection of
 362 images before August 5 were too obscured by clouds or did not show this feature. By
 363 September 6, we see the feature fading from the satellite image. Note that this feature is
 364 centered 0.2 degrees of latitude south of tongue that we observe deeper in the water column,
 365 again indicating that there is depth-dependent structure in the feature.

366 4 Summary and Discussion

367 The intensive sampling discussed here has demonstrated a few important features of
 368 the South Vancouver Island Shelf. The Juan de Fuca Eddy water is readily identified as
 369 falling along a mixing line in $\theta - S$ space, compared with offshore water that was warmer and
 370 saltier (high-spice anomaly). There was not strong evidence of the EDDY being supplied by
 371 water moving up the Spur Canyon during our observations, but the Spur Canyon was a site
 372 of hydraulic cross-canyon flows in which we infer significant mixing has occurred. There is a
 373 sharp and persistent temperature-salinity compensated front between offshore water and the
 374 partially mixed EDDY water. Finally, upstream of the EDDY, water in the equatorward shelf
 375 current has intermediate spice anomaly, and is seen to separate from the shelf at the point
 376 of an abrupt bend in an underwater bank. The water mass crosses isobaths and is ejected
 377 into the interior. This separation event can also be observed from satellite measurements
 378 of sea surface temperature and chlorophyll. Thus the water that is offshore of the EDDY
 379 appears to have been brought onto the shelf in exchange for the offshore ejection of shelf
 380 water via this tongue.

381 4.1 Age and source of the EDDY water

382 The source of water and formation mechanism of the Juan de Fuca Eddy has received
 383 substantial attention, however, the observations of EDDY waters being found along a tight
 384 mixing line in $\theta - S$ space has not previously been noted. The deepest water in the EDDY
 385 could originate along the $\theta - S$ line from approximately 5.5°C to 7.5°C (Fig. 4a), which in
 386 the open ocean spans depths from 420 m to 70 m. Mackas et al. (1987) attempted to
 387 determine the origin of the water by including oxygen as a third variable to resolve the
 388 ambiguous $\theta - S$ relation. However, as Fig. 4b makes clear, oxygen does not appear to be
 389 a conserved property in the EDDY, with concentrations up to 150 $\mu\text{mol kg}^{-1}$ lower in the
 390 EDDY than the water found offshore, and in a way that definitely cannot be the result of
 391 conservative mixing. As a best guess, if the water in the deepest part of the EDDY came
 392 from a vertical mixture of the water at 26.5 kg m^{-3} and an equal distance down in density
 393 space of 26.7 kg m^{-3} , then the deepest water in the EDDY may be coming from a depth of

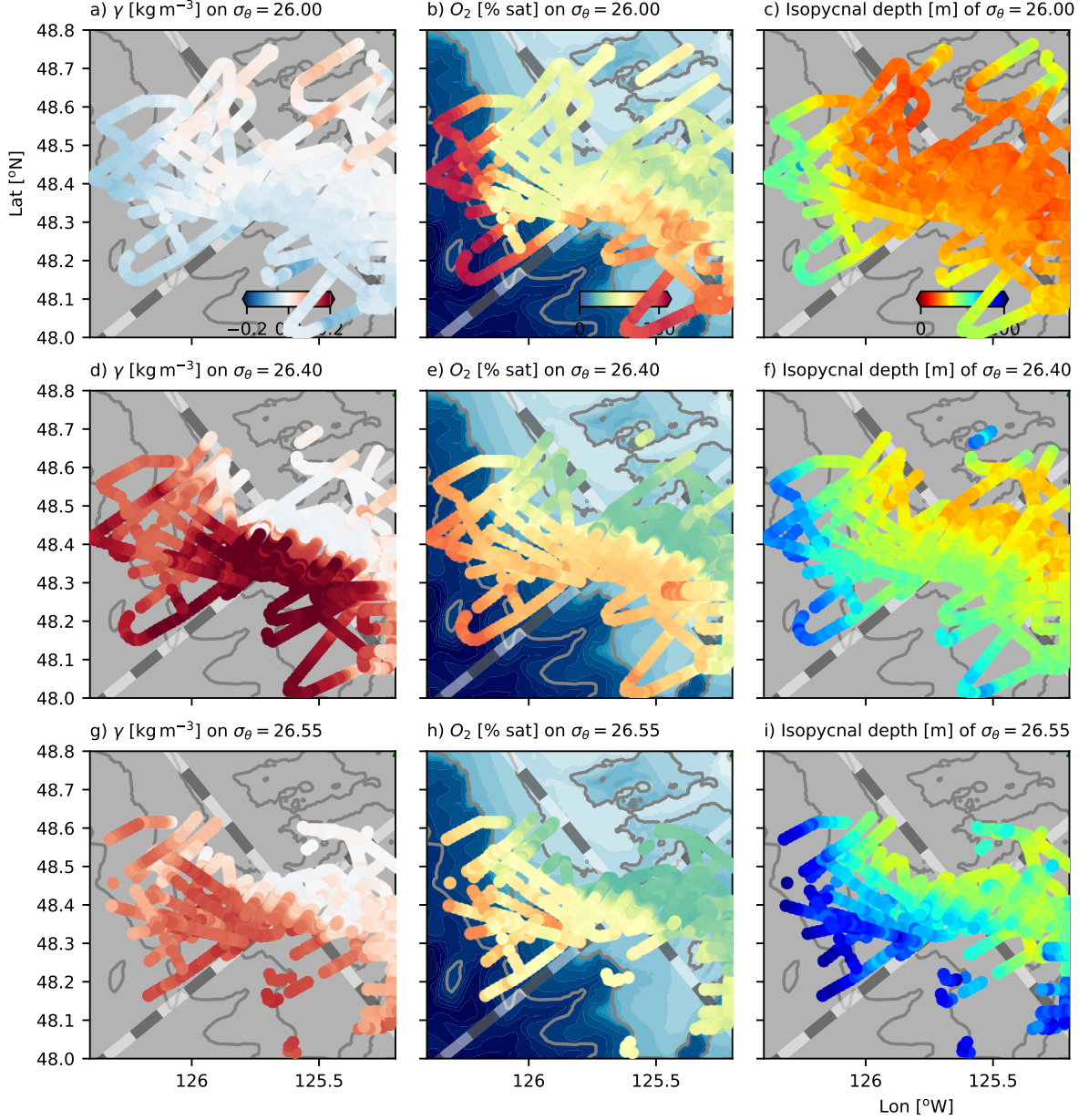


Figure 12. Isopycnal slices of the MVP data showing the vertical structure of the water separating from the shelf, with the first row along 25.5 kg m^{-3} , second along 26.4 kg m^{-3} , and the third at 26.6 kg m^{-3} . First column is the spice anomaly, second is oxygen saturation, and the last column is depth of each isopycnal.

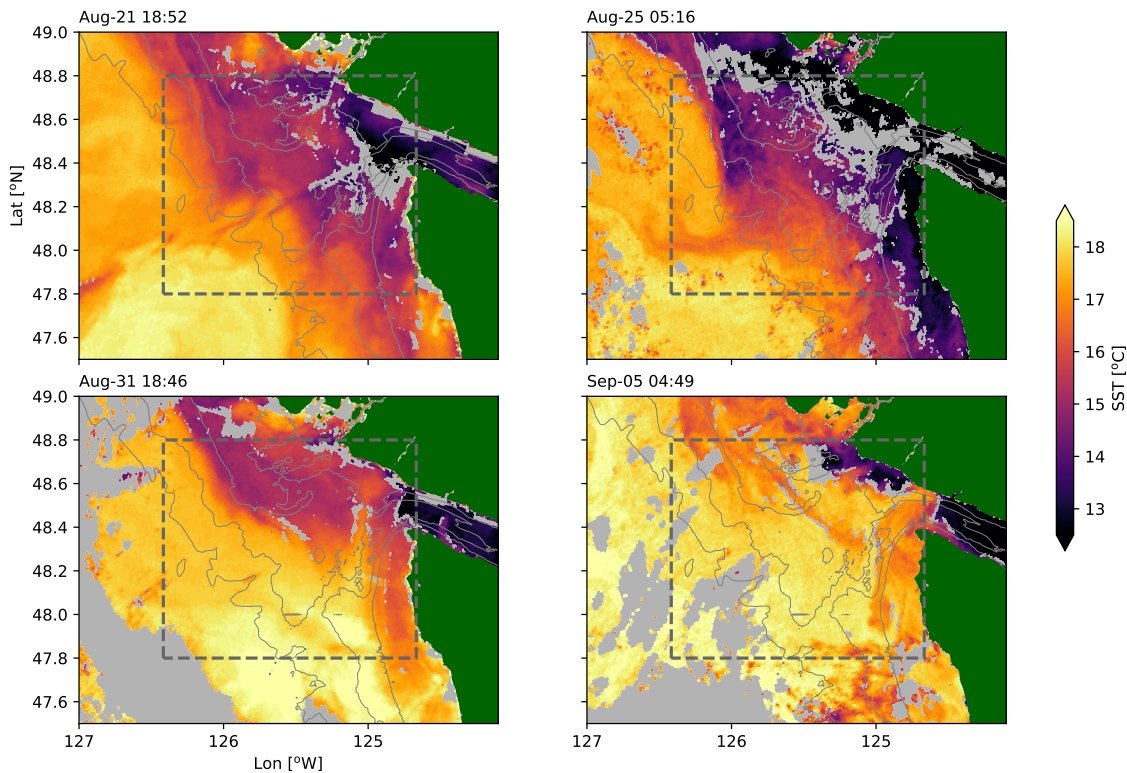


Figure 13. Sea surface temperature snapshots from the observation period. Grey areas are clouds; dashed gray line is the study area. Depths are contoured in thin gray lines at 200, 150 and 100 m. (OSI SAF, 2015)

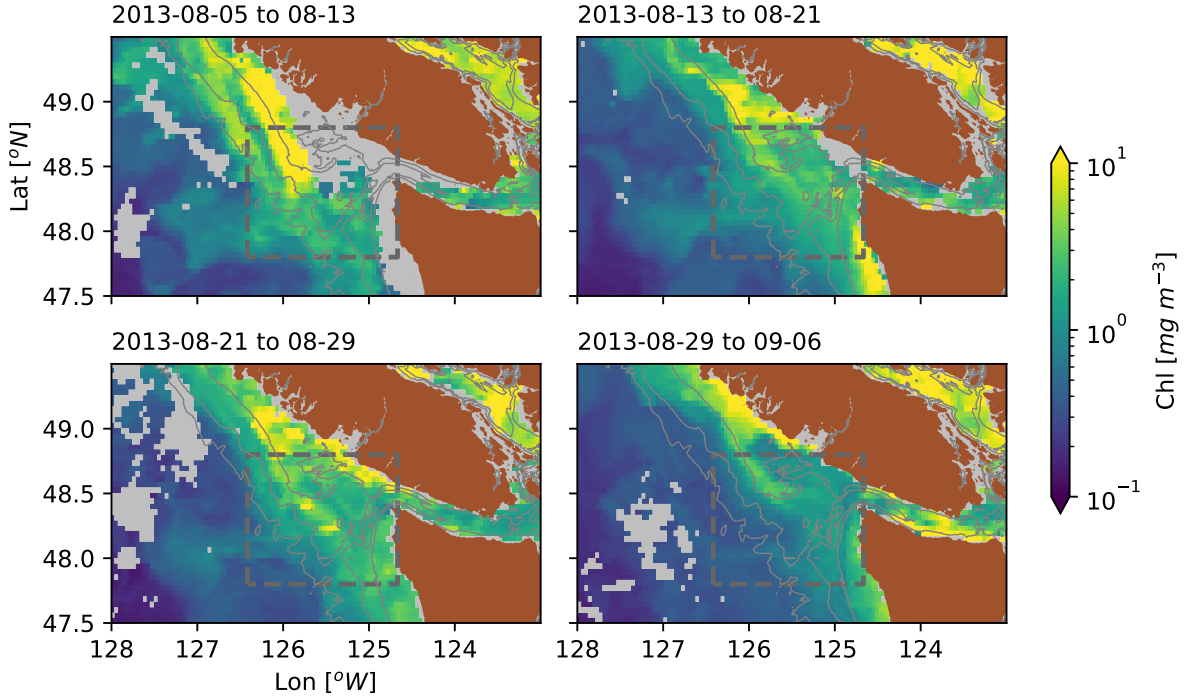


Figure 14. Surface chlorophyll density estimated from ocean color (Hu et al., 2012; NASA Ocean Biology Processing Group, 2017) over 8-day windows in 4-km bins. Gray regions had too many clouds to compute averages.

250 m. This is a typical upwelling depth for coastal flows, and may not require extra input up the Spur Canyon as posited by Freeland and Denman (1982).

We found little evidence of flow up the Spur Canyon or, if there is, then the mixing in the canyon is intense enough to remove the θ - S signature of offshore water within 20 km of the canyon mouth (Fig. 9). We did find substantial evidence of mixing in the canyon, but the primary pathway of high-salinity water into the canyon appears to be due to tidal flow over the banks on the west side (Fig. 10), rather than flow up the canyon. However, it is worthy of note that upwelling winds had ceased at the point of these observations (Fig. 2), so the offshore surface pressure gradient may be reduced, leading to reduced ageostrophic upwelling in the canyon. Whether the cessation of winds would also lead to a reduction of the low sea level height in the center of the EDDY that may drive up-canyon flow is an open question.

There is evidence of aging of the water in the EDDY between late spring and late summer (Fig. 3), with a reduction of oxygen in the EDDY over this time span. If we posited that the reduction was all in the same water, then the oxygen consumption rate over the time between the late-May and early September cruises would be on the order of $0.5 \mu\text{mol kg}^{-1}\text{d}^{-1}$. This is on the low side of estimates of apparent oxygen utilization rates in continental upwelling systems, which are between 1 and $5 \mu\text{mol kg}^{-1}\text{d}^{-1}$ (Dortch et al., 1994; Connolly et al., 2010). So it seems likely that the EDDY has exchange with the surrounding water. Note that during the May cruise, the water in the EDDY is slightly cooler than the mixing line, and during the September cruise is slightly warmer than the mixing line, further evidence that the water in the EDDY is evolving seasonally (Fig. 3e,k). This is consistent with findings on the Oregon shelf where physical processes are thought to account for 55-70% of changes in dissolved oxygen concentrations (Adams et al., 2013). Definitively

418 identifying the exchange mechanisms into the EDDY is challenging from this data set. The
 419 offshore front does not appear to have much exchange, however as noted above there does
 420 appear to be strong tidal flows and mixing over the submarine banks that can transport
 421 more oxygenated water into the EDDY. Further, the Vancouver Island Coastal Current is
 422 oxygen-rich and has a much less sharp front than the offshore front (Fig. 11), and is a likely
 423 source of oxygen to the EDDY.

424 The water is mixed enough in the EDDY that it falls along a mixing line, though it
 425 remains vertically stratified. The amount of homogenization is such that either the mixing is
 426 very strong, or the water is retained in the EDDY for a long time. The amount of turbulence
 427 required to homogenize 100 m of water over 90 days is $\kappa \approx 10^{-3} \text{ m}^2 \text{s}^{-1}$. Given that the
 428 diffusivity implied in the cross-channel surveys was on the order of $\kappa_\rho = 0.5\text{--}5 \text{ m}^2 \text{s}^{-1}$, this
 429 number is not outrageous if we think that such high dissipation is found in 0.2–0.02% of
 430 the water column. We can more carefully quantify this by considering a synthetic profile or
 431 temperature and salinity based on an offshore profile, extrapolated from the bottom of the
 432 200-m cast to 250 m, assuming that the temperature and salinity at 250 m are 6.2 [°C] and
 433 34 psu respectively (Fig. 15). Water at the offshore station was warmer than onshore, so
 434 the profile was also linearly interpolated to a surface value of (12 °C, 31.6 psu). The profile
 435 was then linearly compressed into a depth range of 150 m representative of the shelf depth
 436 in the dense pool, and subjected to mixing with a constant diffusivity of $\kappa = 10^{-3} \text{ m}^2 \text{s}^{-1}$,
 437 with the surface and bottom values pinned under the assumption that the near-bottom
 438 source and surface waters are replenished from a large reservoir. In this calculation, the
 439 T-S relationship does not approach a straight line until after approximately 60–100 days, or
 440 until the mixing affects a vertical length scale of $\lambda = (\tau\kappa)^{1/2} \gtrsim 70 \text{ m}$.

441 Combined with the oxygen observations, the implication is that the water in the EDDY
 442 likely experiences exchange with the outside water, but at a very modest rate. In terms of a
 443 volume flux, we might estimate the EDDY area as 900 km^2 , over 100 m depth, so that 100-d
 444 residence time corresponds to a transport of $10^4 \text{ m}^3 \text{s}^{-1}$, which is remarkably weak for the
 445 transport in and out of such a large area.

446 The sharpness of the front with the EDDY and the offshore water is intriguing. It was
 447 persistent for the duration of our detailed survey (Fig. 8), and, so far as we can tell with
 448 the limited resolution of the hydrographic surveys, was present during the bracketing La
 449 Perouse cruises. There is not any substantial bathymetry blocking the onshore incursion of
 450 water at this location, so there must be a dynamic barrier.

451 Numerical simulations of this region reported by (Sahu et al., 2022) using a NEMO
 452 36th-degree regional model contained relatively rapid exchange between the deep EDDY
 453 water and the rest of the coastal ocean. The region where the EDDY resides has velocities
 454 equal or greater than other parts of the shelf, and water has an approximate residence time
 455 of less than 20 days. The EDDY water in the model does develop a distinct θ -S signature,
 456 but not along a sharp mixing line as observed. It also has a front with the offshore water,
 457 but the front is substantially wider than that observed here. Overall it seems that the
 458 model sees stronger cross-shelf advection than are apparent in these observations, though
 459 the reason for this will require further study.

460 Overall, it would be an improvement to our understanding of the EDDY if we could
 461 sample the shelf more persistently. The EDDY was already well-formed by the May La
 462 Perouse cruise, and seems to evolve slowly during that time. Capturing its formation,
 463 presumably earlier in the spring, as well as its evolution through the year, would be valuable
 464 in understanding retention and exchange on this productive part of the shelf.

465 4.2 Offshore exchange of shelf water

466 The displacement of shelf water from La Perouse Bank is a dramatic departure from
 467 geostrophically balanced isobath-following flow. Eddies have been known to separate from

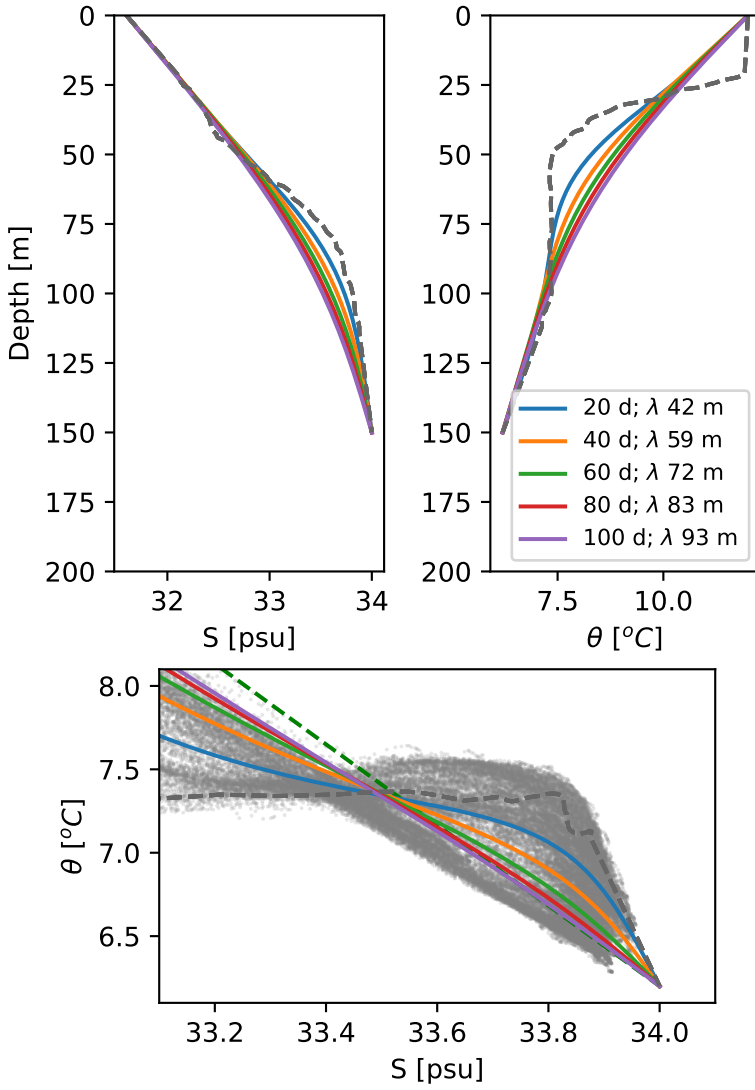


Figure 15. Mixing model assuming constant eddy diffusivity of $\kappa = 10^{-3} \text{ m}^2 \text{s}^{-1}$ acting on an offshore temperature and salinity profiles compressed from 250 thick to 150 m thick (grey dashed lines). Profiles are pinned to the deep $\theta - S$ value at (34 psu, 6.2 °C), and a shallow one at (31.6 psu, 12 °C). The green dashed line is the mixing line defined in the text.

468 irregular coastal topography, both at the surface (Barth et al., 2000) and deeper in the
 469 water column (Pelland et al., 2013). It has been recognized that instabilities lead to exchange
 470 between the open ocean and the shelf at this location (Ikeda & Emery, 1984, 1984). However,
 471 observations of the wholesale replacement of shelf water by a new water mass from offshore
 472 are relatively rare. In the observations presented here, it is clear that water from as deep as
 473 150 m is separating from the shelf and moving offshore (Fig. 8, Fig. 12).

474 Satellite imagery shows that there is often exchange between coastal and deep waters
 475 along the Vancouver Island shelf (Fig. 16). Most years there are three of four large filaments
 476 from the shelf into the open ocean, many of them over 100 km long. This length scale is
 477 longer than the 60 km inferred for this region by Ikeda et al. (1984) using a four-layer
 478 instability analysis. It is possible that there is spatial locking of these features, with a
 479 persistent separation at the north tip of Vancouver Island, and a strong tendency for one
 480 at 49.5 N. There is also evidence of separation events in most of the years, with 2011
 481 being the only clear exception. General baroclinic instability of the upwelling front is a
 482 possible mechanism to drive offshore exchange (Ikeda et al., 1984; Durski & Allen, 2005),
 483 but this tends to be shallow, with smaller-scale instabilities that will not extend as far into
 484 the interior ocean as observed here. Rather it seems likely that the topographic change
 485 engendered by the sudden turn to the east of La Perouse Bank catalyses a larger scale
 486 instability at this location. In California most of the cold filaments observed appear to be
 487 catalyzed by headlands and underwater topography (Strub et al., 1991), though modelling
 488 studies find instabilities are possible even in two-dimensional flows (Pierce et al., 1991).
 489 Durski and Allen (2005), when modelling the Oregon shelf, found that including realistic
 490 shelf bathymetry catalyzed intermittent large-scale instabilities, a finding that is deemed
 491 likely to apply at other coastal locations (Battieen, 1997).

492 Large-scale mixing between the shelf and open ocean has been evident since the satellite
 493 era. Here we demonstrate that in the Vancouver Island shelf the flow is originating on the
 494 shelf and separating from the bathymetry and being injected into the interior. A similar
 495 observation was made by Barth et al. (2000) downstream of Cape Blanco, Oregon, where
 496 the coastal current was observed to detach from the shelf in the lee of the cape and flow into
 497 the interior. They hypothesized that as the current moved offshore, it deepened, stretching
 498 isopycnals and creating cyclonic relative vorticity that would tend to push the current back
 499 onshelf, but then it was caught in the undercurrent and stalled, being pushed offshore. It is
 500 also possible that coastally trapped waves in the region experience a hydraulic control, and
 501 these separation events are part of the response (Dale & Barth, 2001).

502 Regardless of the dynamics of the separation events, the offshore transport can be
 503 substantial. If we assume the coastal current is approximately 0.1 m s^{-1} over 100 m in the
 504 vertical and 20 km in the horizontal, it represents 0.2 Sv of nutrient- and chlorophyll-rich
 505 shelf water transported offshore. Sometimes the along-shelf currents are substantially larger
 506 than this (Thomson & Krassovski, 2015) reaching 0.4 m s^{-1} . Our observations are a finer-
 507 detailed representation of the kind of cross-shore transports inferred by Mackas and Yelland
 508 (1999) from hydrographic surveys, and definitively show that this water can originate from
 509 the shelf from relatively deep depths and be transported offshore. We do not have velocity
 510 measurements for the water that replaces it, but assuming that water also flows along-shelf,
 511 these separation events are associated with a large replacement of shelf water with offshore
 512 water at this location. This emphasizes the importance of three dimensional observations
 513 and modeling of cross-shelf dynamics when thinking about physical and biological processes
 514 on the shelf.

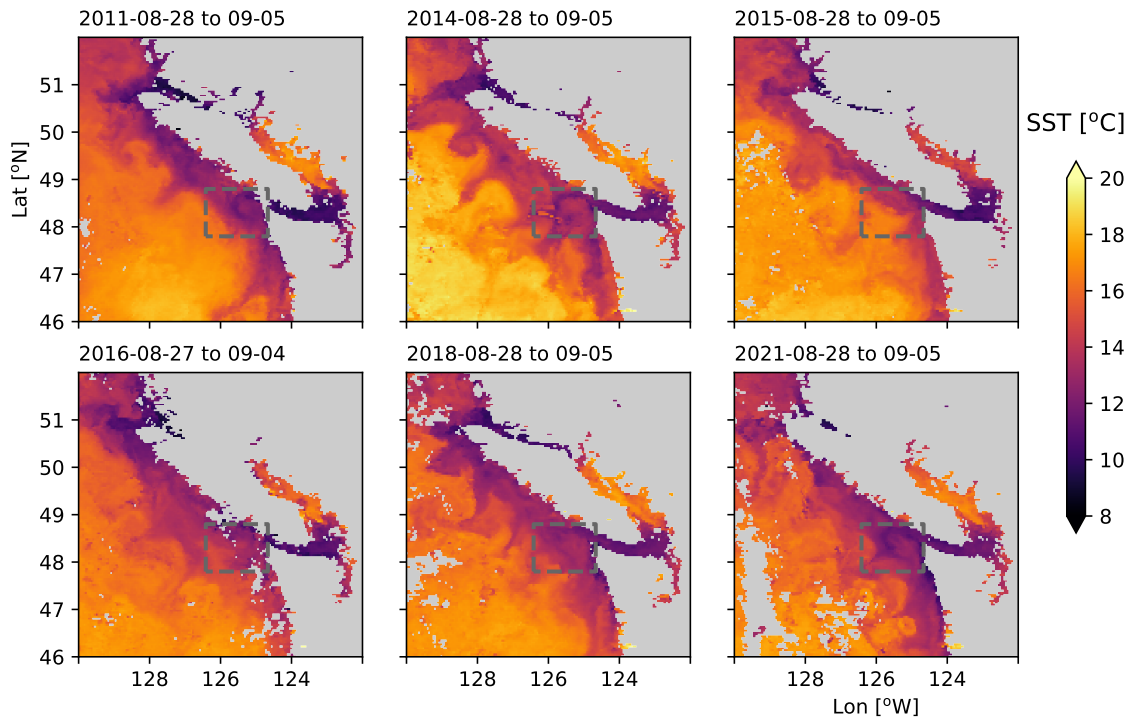


Figure 16. Available late-August sea-surface temperature from 8-day composites, 2011 to 2021 (NASA Ocean Biology Processing Group, 2019); missing years had too much cloud cover or no satellite coverage.

515 Open Research

516 Derived data files (1-m vertical binned CTD files) and analysis scripts are available at
 517 <https://ocean-physics.seos.uvic.ca/~jklymak/PW13DataAnalysis/>. Raw CTD data
 518 is available on request. Data was processed using a scientific python toolchain as listed at
 519 <https://ocean-physics.seos.uvic.ca/~jklymak/PW13DataAnalysis/environment.yml>;
 520 major components include xarray (Hoyer & Hamman, 2017), numpy (Harris et al., 2020),
 521 and Matplotlib (Caswell et al., 2022), but those all leverage many smaller but vital projects.

522 Acknowledgments

523
 524 Thank you to the officers and crew of the R/V Falkor and the Schmidt Foundation
 525 for funding the seagoing component of the cruise. Thank you to Richard Dewey, Benjamin
 526 Schieffe, and Rowan Fox for efforts during the cruise. Jack Barth and an anonymous re-
 527 viewer provided valuable feedback on the manuscript. Klymak was supported by NSERC
 528 Discovery grant RGPIN-2017-04050 and a Canadian Foundation for Innovation Leading
 529 Edge Fund grant 36109, Allen was supported by NSERC Discovery grant RGPIN-105694-
 530 11, and Waterman was supported by NSERC Discovery grant RGPIN-2020-05799.

531 References

- 532 Adams, K. A., Barth, J. A., & Chan, F. (2013). Temporal variability of near-bottom dis-
 533 solved oxygen during upwelling off central Oregon. *J. Geophys. Res. Oceans*, 118(10),
 534 4839–4854. doi: 10.1002/jgrc.20361
- 535 Barth, J. A., Pierce, S. D., & Smith, R. L. (2000). A separating coastal upwelling jet at
 536 Cape Blanco, Oregon and its connection to the California Current system. *Deep Sea*
 537 *Res. II*, 47(5–6), 783 - 810. doi: [http://dx.doi.org/10.1016/S0967-0645\(99\)00127-7](http://dx.doi.org/10.1016/S0967-0645(99)00127-7)
- 538 Batteen, M. L. (1997). Wind-forced modeling studies of currents, meanders, and eddies in
 539 the California Current system. *J. Geophys. Res.*, 102(C1), 985–1010. doi: 10.1029/
 540 96jc02803
- 541 Brink, K. (2016). Cross-shelf exchange. *Annu. Rev. Mar. Sci.*, 8(1), 59–78. doi: 10.1146/
 542 annurev-marine-010814-015717
- 543 Castelao, R. M., & Barth, J. A. (2007, nov). The role of wind stress curl in jet separation
 544 at a cape. *J. Phys. Oceanogr.*, 37(11), 2652–2671. doi: 10.1175/2007jpo3679.1
- 545 Caswell, T. A., Lee, A., Droettboom, M., De Andrade, E. S., Hoffmann, T., Klymak, J.,
 546 ... Kniazev, N. (2022). *matplotlib/matplotlib: Rel: v3.6.0*. Zenodo. Retrieved from
 547 <https://zenodo.org/record/7084615> doi: 10.5281/ZENODO.7084615
- 548 Connolly, T. P., Hickey, B. M., Geier, S. L., & Cochlan, W. P. (2010, mar). Processes
 549 influencing seasonal hypoxia in the northern California current system. *J. Geophys.*
 550 *Res.*, 115(C3). Retrieved from <https://doi.org/10.1029%2F2009jc005283> doi:
 551 10.1029/2009jc005283
- 552 Dale, A. C., & Barth, J. A. (2001, jan). The hydraulics of an evolving upwelling jet flowing
 553 around a cape. *Journal of Physical Oceanography*, 31(1), 226–243. doi: 10.1175/
 554 1520-0485(2001)031(0226:thoaeu)2.0.co;2
- 555 D'Asaro, E. (1988). Generation of submesoscale vortices: A new mechanism. *J. Geophys.*
 556 *Res.*, 93, 6685–6693.
- 557 D'Asaro, E. A., Shcherbina, A. Y., Klymak, J. M., Molemaker, J., Novelli, G., Guigand,
 558 C. M., ... Özgökmen, T. M. (2018, Jan). Ocean convergence and the dispersion of
 559 flotsam. *Proc. Natl. Acad. Sci. U.S.A.*, 201718453. doi: 10.1073/pnas.1718453115
- 560 Dewey, R. K., & Crawford, W. R. (1988). Bottom stress estimates from vertical dissipation
 561 rate profiles on the continental shelf. *J. Phys. Oceanogr.*, 18, 1167–1177.
- 562 DFO. (2022). *Marine environmental data section archive, buoy c46206*. Ecosystem
 563 and Oceans Science, Department of Fisheries and Oceans Canada. Retrieved from
 564 <https://meds-sdmm.dfo-mpo.gc.ca>

- Dortch, Q., Rabalais, N. N., Turner, R. E., & Rowe, G. T. (1994, dec). Respiration rates and hypoxia on the Louisiana shelf. *Estuaries*, 17(4), 862. doi: 10.2307/1352754
- Durski, S. M., & Allen, J. S. (2005). Finite-amplitude evolution of instabilities associated with the coastal upwelling front. *J. Phys. Oceanogr.*, 35(9), 1606–1628. doi: 10.1175/jpo2762.1
- Engida, Z., Monahan, A., Ianson, D., & Thomson, R. E. (2016). Remote forcing of subsurface currents and temperatures near the northern limit of the California Current system. *J. Geophys. Res.*, 121(10), 7244–7262. doi: 10.1002/2016jc011880
- Foreman, M. G. G., Callendar, W., MacFadyen, A., Hickey, B. M., Thomson, R. E., & Lorenzo, E. D. (2008). Modeling the generation of the Juan de Fuca Eddy. *J. Geophys. Res.*, 113(C3). doi: 10.1029/2006jc004082
- Freeland, H., & Denman, K. (1982). A topographically controlled upwelling ceter off southern Vancouver Island. *J. Mar. Res.*, 40(4), 1069–1093.
- Freeland, H., & McIntosh, P. (1989). The vorticity balance on the southern British Columbia continental shelf. *Atmosphere–Ocean*, 27(4), 643–657.
- Harris, C. R., Millman, K. J., van der Walt, S. J., Gommers, R., Virtanen, P., Cournapeau, D., ... Oliphant, T. E. (2020, sep). Array programming with NumPy. *Nature*, 585(7825), 357–362. Retrieved from <https://doi.org/10.1038/s41586-020-2649-2> doi: 10.1038/s41586-020-2649-2
- Hickey, B., Thomson, R., Yih, H., & LeBlond, P. (1991). Velocity and temperature fluctuations in a buoyancy-driven current off Vancouver Island. *J. Geophys. Res.*, 96(C6), 10,507–10,538.
- Hoyer, S., & Hamman, J. (2017, apr). xarray: N-d labeled arrays and datasets in python. *Journal of Open Research Software*, 5(1), 10. Retrieved from <https://doi.org/10.5334/jors.148> doi: 10.5334/jors.148
- Hu, C., Lee, Z., & Franz, B. (2012). Chlorophyll a algorithms for oligotrophic oceans: A novel approach based on three-band reflectance difference. *J. Geophys. Res.*, 117(C1). doi: 10.1029/2011jc007395
- Ikeda, M., & Emery, W. J. (1984). A continental shelf upwelling event off Vancouver Island as revealed by satellite infrared imagery. *J. Mar. Res.*, 42(2), 303–317. doi: 10.1357/002224084788502774
- Ikeda, M., Mysak, L. A., & Emery, W. J. (1984). Observation and modeling of satellite-sensed meanders and eddies off Vancouver Island. *J. Phys. Oceanogr.*, 14(1), 3–21. doi: 10.1175/1520-0485(1984)014<0003:oamoss>2.0.co;2
- Klymak, J. M., Crawford, W., Alford, M. H., MacKinnon, J. A., & Pinkel, R. (2015). Along-isopycnal variability of spice in the North Pacific. *J. Geophys. Res.*, 2169–9291. doi: 10.1002/2013JC009421
- Klymak, J. M., Shearman, R. K., Gula, J., Lee, C. M., D'Asaro, E. A., Thomas, L. N., ... others (2016). Submesoscale streamers exchange water on the north wall of the Gulf Stream. *Geophys. Res. Lett.*. doi: 10.1002/2015GL067152
- MacFadyen, A., & Hickey, B. M. (2010). Generation and evolution of a topographically linked, mesoscale eddy under steady and variable wind-forcing. *Cont. Shelf Res.*, 30(13), 1387–1402. doi: 10.1016/j.csr.2010.04.001
- Mackas, D. L., Denman, K. L., & Bennett, A. F. (1987). Least squares multiple tracer analysis of water mass composition. *J. Geophys. Res.*, 92(C3), 2907–2918.
- Mackas, D. L., & Yelland, D. R. (1999, nov). Horizontal flux of nutrients and plankton across and along the British Columbia continental margin. *Deep Sea Res. II*, 46(11–12), 2941–2967. doi: 10.1016/s0967-0645(99)00089-2
- NASA Ocean Biology Processing Group. (2017). *MODIS-aqua level 3 mapped chlorophyll data version r2018.0*. NASA Ocean Biology DAAC. Retrieved from <https://oceancolor.gsfc.nasa.gov/data/10.5067/AQUA/MODIS/L3M/CHL/2018> doi: 10.5067/AQUA/MODIS/L3M/CHL/2018
- NASA Ocean Biology Processing Group. (2019). *MODIS-aqua level 3 mapped SST data version r2019.0*. NASA Ocean Biology DAAC. Retrieved from https://oceandata.sci.gsfc.nasa.gov/ob/getfile/AQUA_MODIS

- 620 OSI SAF. (2015). *GHRSSST level 2p sub-skin sea surface temperature from the Advanced*
 621 *Very High Resolution Radiometer (AVHRR) on Metop satellites (currently Metop-A)*
 622 *(GDS V2) produced by OSI SAF.* NASA Physical Oceanography DAAC. Retrieved
 623 from https://podaac.jpl.nasa.gov/dataset/AVHRR_SST_METOP_A-OSISAF-L2P-v1
 624 .0 doi: 10.5067/GHAMA-2PO02
- 625 Pelland, N. A., Eriksen, C. C., & Lee, C. M. (2013). Subthermocline eddies over the
 626 Washington continental slope as observed by Seagliders, 2003–09. *J. Phys. Oceanogr.*.
 627 doi: 10.1175/JPO-D-12-086.1
- 628 Pierce, S. D., Allen, J. S., & Walstad, L. J. (1991). Dynamics of the coastal transition
 629 zone jet: 1. linear stability analysis. *J. Geophys. Res.*, 96(C8), 14979. Retrieved from
 630 <https://doi.org/10.1029/91jc00979> doi: 10.1029/91jc00979
- 631 Relvas, P., & Barton, E. D. (2005). A separated jet and coastal counterflow during upwelling
 632 relaxation off Cape São Vicente (Iberian Peninsula). *Cont. Shelf Res.*, 25(1), 29–49.
 633 doi: 10.1016/j.csr.2004.09.006
- 634 Sahu, S., Allen, S. E., Saldías, G. S., Klymak, J. M., & Zhai, L. (2022, mar). Spatial and
 635 temporal origins of the La Perouse low oxygen pool: A combined lagrangian statistical
 636 approach. *J. Geophys. Res.*, 127(3). doi: 10.1029/2021jc018135
- 637 Strub, P. T., Kosro, P. M., & Huyer, A. (1991). The nature of the cold filaments in
 638 the California current system. *J. Geophys. Res.*, 96(C8), 14743–14768. doi: 10.1029/
 639 91jc01024
- 640 Thomson, R. E., & Gower, J. F. R. (1998). A basin-scale oceanic instability event in the
 641 Gulf of Alaska. *J. Geophys. Res.*, 103(C2), 3033–3040. doi: 10.1029/97jc03220
- 642 Thomson, R. E., Hickey, B. M., & LeBlond, P. H. (1989). The Vancouver Island Coastal
 643 Current: Fisheries barrier and conduit. In R. J. Beamish & G. A. McFarlane (Eds.),
 644 *Effects of ocean variability on recruitment and an evaluation of parameters used in*
 645 *stock assessment models.* Fisheries and Oceans Canada.
- 646 Thomson, R. E., & Krassovski, M. V. (2015, dec). Remote alongshore winds drive variability
 647 of the California Undercurrent off the British Columbia–Washington coast. *J. Geophys.*
 648 *Res.*, 120(12), 8151–8176. doi: 10.1002/2015jc011306
- 649 Weaver, A. J., & Hsieh, W. W. (1987). The influence of buoyancy flux from estuaries
 650 on continental shelf circulation. *J. Phys. Oceanogr.*, 17, 2127–2140. doi: 10.1175/
 651 1520-0485(1987)017<2127:TIOBFF>2.0.CO;2